ACS SyntheticBiology

pubs.acs.org/synthbio Research Article

Caged Activators of Artificial Allosteric Protein Biosensors

Selvakumar Edwardraja,[#] Zhong Guo,[#] Jason Whitfield, Ignacio Retamal Lantadilla, Wayne A. Johnston, Patricia Walden, Claudia E. Vickers, and Kirill Alexandrov*

Cite This: *ACS Synth. Biol.* 2020, 9, 1306–1314 Read Online

ACCESS | Metrics & More | Article Recommendations | Supporting Information

ABSTRACT: The ability of proteins to interconvert unrelated biochemical inputs and outputs underlays most energy and information processing in biology. A common conversion mechanism involves a conformational change of a protein receptor in response to a ligand binding or a covalent modification, leading to allosteric activity modulation of the effector domain. Designing such systems rationally is a central goal of synthetic biology and protein engineering. A two-component sensory system based on the scaffolding of modules in the presence of an analyte is one of the most generalizable biosensor architectures. An inherent problem of such systems is dependence of the response on the absolute and relative concentrations of the components. Here we use the example of two-component sensory systems based on calmodulin-operated synthetic switches to analyze and address this issue. We constructed "caged" versions of the activating domain thereby creating a thermodynamic barrier for spontaneous activation of the system. We demonstrate that the caged biosensor architectures could operate at concentrations spanning 3 orders of magnitude and are applicable to electrochemical, luminescent, and fluorescent two-component biosensors. We analyzed the activation kinetics of the caged biosensors and determined that the core allosteric switch is likely to be the rate limiting component of the system. These findings provide guidance for predictable engineering of robust sensory systems with inputs and outputs of choice.

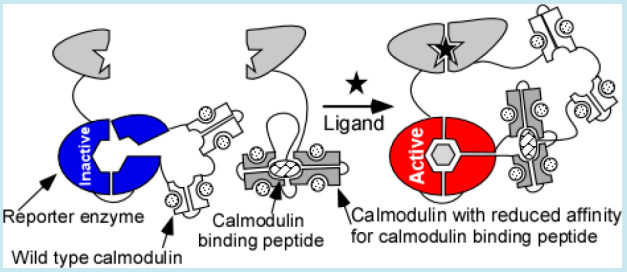

Allosteric regulation of proteins controls every aspect of information and energy processing in biological systems.[1,2] In many cases it enables direct coupling of multiple signaling and metabolic pathways through allosteric hub molecules, endowing the resulting systems with complex and elastic regulation. Not surprising, understanding and engineering allosterically regulated proteins is a key objective of protein sciences and synthetic biology. A number of studies combined experimental and computational approaches to construct allosteric switches from constitutively active enzymes. Domain insertion is one of the commonly used and most successful approaches[3,4] whereby a ligand binding domain that undergoes a conformational change in response to binding is genetically inserted into a distortion-sensitive site of the reporter domain. For example, Solute Binding Proteins that undergo large conformational changes in response to ligand-binding were successfully used to construct biosensors of small molecules.[5] However, this approach inherently relies on the availability of receptor domains with large conformational changes, yet only a fraction of ligand binding proteins undergo discernible conformational change.[6,7] As a result, binding domains that display only local structural rearrangements, such as antibodies or their synthetic analogues, are not well suited for the purpose of allosteric biosensor construction. Furthermore, the conformational coupling is an empirical process that typically requires significant optimization of both insertion sites and linkers connecting the receptor and reporter domains.[8−10]

We and others demonstrated that insertion of calmodulin (CaM) into rationally selected sites of the reporter domains such as fluorescent proteins, NanoLuciferase, dehydrofolate reductase, glucose dehydrogenase (GDH), and β-lactamase converts them into allosteric receptors of calmodulin binding peptide (CaM-BP).[11,12] In some cases the dynamic range of the resulting switch modules was as large as 200 fold.[12] The resulting switches can be integrated into higher order signaling systems in which ligand mediated association of the low affinity variant of CaM-BP with the allosteric switch module results in reporter activation (Figure 1). We constructed a range of two-component biosensors based on different reporters, thereby demonstrating that the approach is generally applicable. The developed biosensors could detect analytes such as proteins and small molecules in complex biological samples with an accuracy equal of that of the current diagnostic methods.[12]

Unlike fully integrated natural or artificial allosteric proteins in which ligand binding is actuated through intramolecular conformational changes, the two-component biosensors are largely concentration driven systems that are much less

Received: December 9, 2019
Published: April 27, 2020

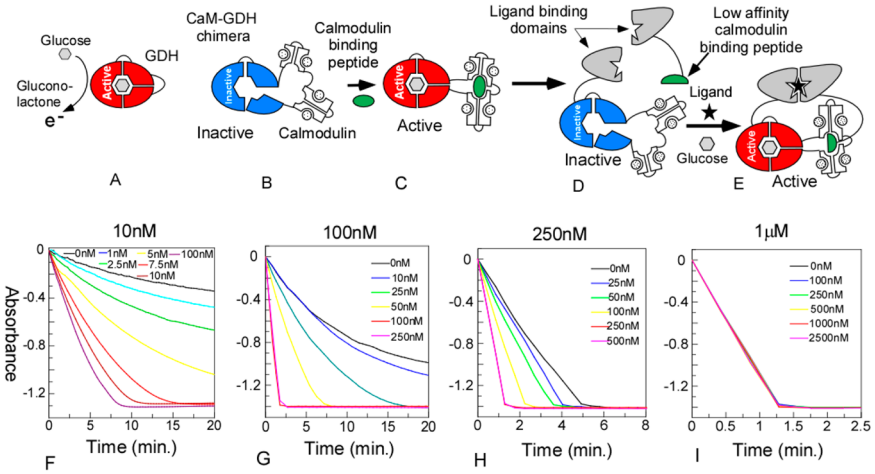

Figure 1. Design and functional mechanism of calmodulin-operated artificial allosteric protein switches and thereon-based two-component biosensors. (A) Schematic representation of PQQ−glucose dehydrogenase. The hexagon represents a glucose molecule and e- represents the generated electrons. (B) Schematic representation of calmodulin-GDH chimera and (C) the proposed mechanism of its activation by a calmodulin binding peptide (CaM-BP). (D−E) Schematic representation of GDH-CaM chimera-based two-component biosensor where analyte scaffolds the subunits of the biosensors leading to allosteric switching and activation of the reporter enzyme. (F) GDH activity of 10 nM solution of CaM-GDH-FKBP and 15 nM of FRB complex fused to low affinity version of CaM-BP in the presence of increasing concentrations of rapamycin. The activity of the enzyme was monitored by changes in the absorption of electron accepting dye dichlorophenolindophenol in the presence of 0.6 mM electron mediator phenazine methosulfate, 20 mM of glucose, and 1 mM $CaCl_2$. (G) As in graph F but using 100 nM solution of CaM-GDH-FKBP and 150 nM of activator; (H) as in graph F but using 250 nM solution of CaM-GDH-FKBP and 350 nM of the activator. The concentration of PQQ was maintained at 1 nM to keep the reaction rates in the measurable range. (I) As in graph H but using 1 μM solution of CaM-GDH-FKBP and 1.5 μM of the activator. The concentration of rapamycin used for titration is shown in the inset.

sensitive to the relative orientation of the binding domains and the target. While this makes construction of such biosensors more predictable, it inevitably creates the dependence of the system's output on the relative and absolute concentration of the biosensor components.

In the present study we propose a solution to the concentration dependency of two-component allosteric biosensors by introducing "caged" versions of CaM-BP-based activators that display reduced concentration sensitivity and improved dynamic range. We demonstrate that this approach is generic and can be used to construct concentration tolerant two-component systems with different outputs.

RESULTS

Concentration Dependence of Two-Component Allosteric Biosensors. To test the concentration dependence of the previously designed two-component biosensor architecture we monitored the activity of a glucose dehydrogenase (GDH)-based biosensor of macrocyclic peptide rapamycin at the different concentrations of biosensor components and the ligand.[12] In this biosensor the ligand stimulates dimerization of FKBP tagged CaM-GDH with a FRB fusion protein linked to a low affinity variant of CaM-BP. The interaction of CaM-BP with calmodulin-GDH chimera leads to a conformational change and activation of the latter. When the performance of the biosensors was tested at the increased concentrations of the components, we observed an increase of the background activation and a decrease in signal's change from approximately 7.5 fold at 10 nM to no response at 1 μM (Figure 1F−I). This is consistent with the functional mechanism of the biosensor, where at higher concentrations of the activation component its equilibrium with the reporter domain shifts further toward the complex as evidenced by the data presented in Figure S2. As a result utilization of this two-component biosensor architecture requires careful balancing of the biosensor component's affinities and concentrations.

Design, Construction, and Testing of Caged CaM-BP Activators. The inherent dependence of the assay's dynamic range on the analyte concentration complicates deployment of the two-component biosensor both *in vivo* and *in vitro*. We conjectured that creation of a kinetic and thermodynamic barrier between the CaM-BP and its binding site on the reporter component could alleviate the problem by reducing the collision rate of the CaM-BP and its receptor, thereby reducing the spontaneous activation of the latter. This, in principle, could be achieved by supplying a free calmodulin to the system that would associate with the CaM-BP and thus reduce its spontaneous binding to the reporter. However, this would also make the system significantly more complex. Hence, we sought to create a system that had an integrated thermodynamic barrier preventing spontaneous activation of the reporter. With this in mind we redesigned an activating component of the biosensor system by fusing CaM-BP via linker to calmodulin (Figure 2A). In this case no interaction between activating peptide and CaM-GDH is expected to occur due to sequestration of CaM-BP by the caging calmodulin in intermolecular complex. This is expected to remain the case even at high concentrations of the components, as the intramolecular equilibrium would disfavor binding of CaM-BP to calmodulin present in *trans*. The ligand-mediated scaffolding of both components would increase the local concentration of both calmodulin units thereby increasing the K_{on} of CaM-BP interaction with CaM-reporter chimera. The distribution of the peptide between two CaM molecules is expected to be a function of the affinities, length of the linker, and at least to some extent, the arrangement of the domains in space. However, such a system would equilibrate with a rate equal to or slower than the k_{off} of the caged CaM:CaM-BP complex. We, therefore, hypothesized that by reducing the

https://dx.doi.org/10.1021/acssynbio.9b00500
ACS Synth. Biol. 2020, 9, 1306−1314

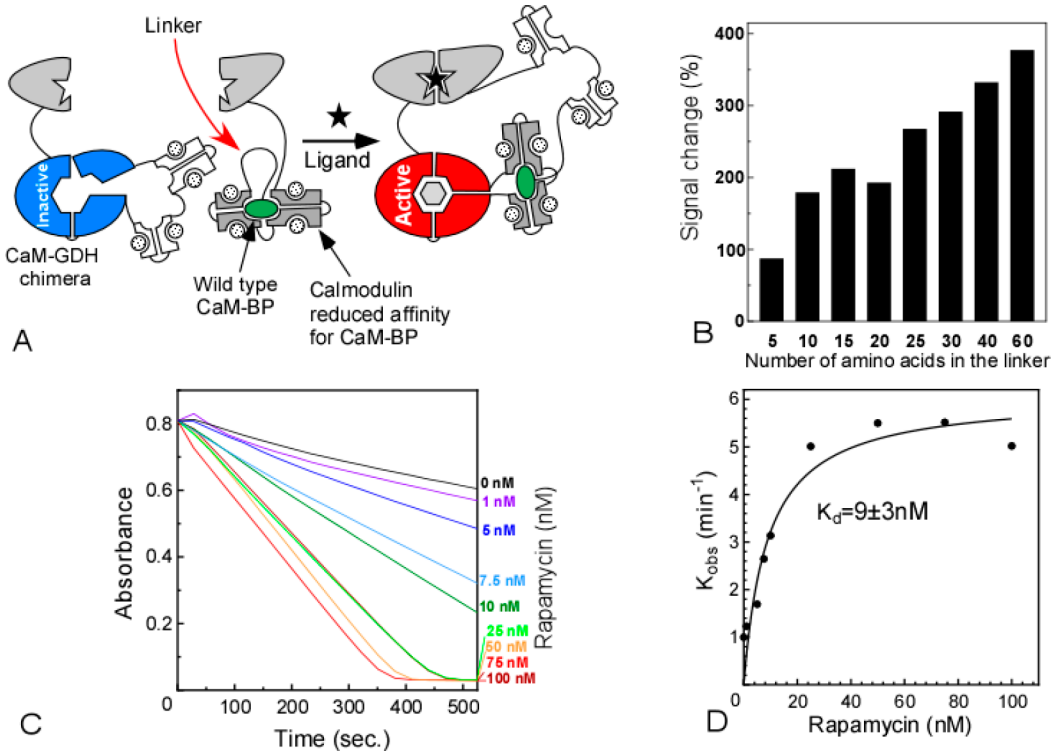

Figure 2. Caged two-component biosensors. (A) Schematic representation of the proposed two-component GDH biosensor based on the allosteric switch unit constructed with caged-CaM-BP activator. Ligand mediated complex formation between ligand binding domains increases the local concentration of the caged-CaM-BP in the proximity of the wild type calmodulin, and relocation of the CaM-BP drives the conformation change of the reporter. The red arrow marks the linker between the CaM-BP and CaM, the length of which was varied. The functional elements are colored as in Figure 1. (B) Effect of the length of the linker between the CaM-BP and calmodulin on the dynamic range of caged two-component rapamycin biosensor. The percentage change represents the increase in signal level between the background activity and the maximal observed signal at saturating concentrations of rapamycin. (C) Activity of mixture of 10 nM of CaM-GDH-FKBP with 2 μM of FRB-lowCaM-M13 with 28 amino acid linker in the presence of the indicated concentrations of rapamycin. (D) Fit of the data shown in C leading to a K_d value of 9.03 ± 3.2 nM. The activity of the enzyme was monitored by changes in absorption of the electron accepting dye dichlorophenolindophenol in the presence of 0.6 mM electron mediator phenazine methosulfate, 20 mM of glucose, and 1 mM $CaCl_2$.

affinity of the CaM:CaM-BP interaction within the fusion, while keeping the affinity of CaM-BP for CaM-GDH reporter constant, would provide a thermodynamic driver for systems activation in the presence of the scaffolding ligand (Figure 2).

To test this idea we first sought to design CaM mutants with reduced affinity for CaM-BP and therefore display rapid dissociation kinetics. To this end we analyzed the crystal structure of human CaM and M13 CaM-BP complex (PDB ID: 2BBM) to identify the residues in the former that could be mutated without compromising the overall interaction. On the basis of our analysis we sought to reduce the hydrophobic interaction between CaM and CaM-BP by introducing F92A, and F141A mutations next to the Ca^{2+} binding loops preceding the EF-3 arm and succeeding the EF-4 arm, respectively. We also designed a L105A mutation aimed to further reduce the hydrophobic interactions with the peptide as well as the E83S located near the hinge region between the N-lobe and C-lobe of calmodulin (Figure S1). We combined these substitutions into two mutant variants of calmodulin: F92A and F141A, as well as F92A, F141A, L105A, and E83S, that we expected to display medium and low affinity for CaM-BP, respectively. The coding sequence of the wild type calmodulin and two mutants was fused to the N-terminus to the wild type M13 CaM-BP sequence via a 12 amino acid flexible linker (Table S1). The combined open reading frames were fused to the coding sequence of the rapamycin binding domain FRB, and the resulting chimeric proteins were expressed in *E. coli* and purified to homogeneity (Figure S3). When the solutions of recombinant CaM-GDH-FKBP and FRB-CaM:CaM-BP variants were mixed, only a low level of GDH activity was observed for the wild type and mutants, even at 2 μM concentration of the activating component (Figure S4). This suggests that CaM-BP peptide is efficiently sequestered by the WT and calmodulin mutants, and collisions of the biosensor components do not lead to its relocation onto CaM-GDH. We next tested if a rapamycin mediated interaction of FRB and FKBP that increases the local concentration of the components is sufficient to override the activation barrier. As expected, the presence of rapamycin ligand induced GDH activity in the case of all constructs with activation being most pronounced in the biosensor based on the low affinity version of calmodulin. However, both the catalytic rate and dynamic range were lower than in the control experiments where free CaM-BP was used (Figure S4). On the basis of the analysis of the structures, we hypothesized that this could be due to steric clashes between two calmodulin modules resulting from constraints introduced by the linker connecting the CaM-BP and mutant calmodulin.

To test the effect of linker length on the efficiency of the activation we produced eight versions of FRB-lowCaM-M13 fusions with linkers ranging from 5 to 60 amino acids (Figure S5). The ability of these variants to activate the GDH activity of the CaM-GDH-FRB fusion in a rapamycin-dependent

https://dx.doi.org/10.1021/acssynbio.9b00500
ACS Synth. Biol. 2020, 9, 1306−1314

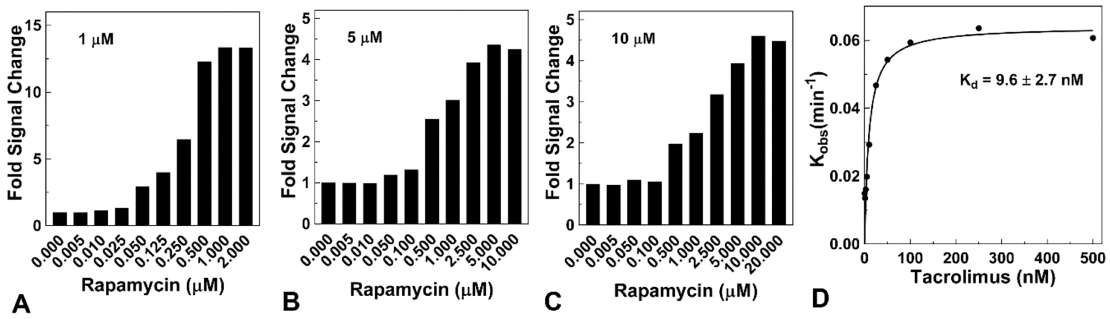

Figure 3. Performance of the caged biosensors at different concentrations of biosensor components. (A) Time-resolved absorption changes reaction containing 1 μM of sensor components in response to the increasing concentrations of rapamycin between 0 and 2 μM. The concentration of the GDH cofactor PQQ was kept at 0.5 nM. (B) As in panel A, but using 5 μM of biosensor components and 0 and 10 μM of rapamycin. (C) Same as in panel A, but using 10 μM of biosensor components and concentration of rapamycin between 0 and 20 μM. The concentration of the GDH cofactor PQQ was kept at 0.1 nM. The fit of the data is shown in Figure S7. (D) Activity of 10 nM of CaM-GDH-FKBP mixed with 1 μM of CaA/CalB-lowCaM-CaM-BP in the presence of the indicated concentrations of tacrolimus. The fit of the data leads to a K_d value of 9.6 ± 2.7 nM.

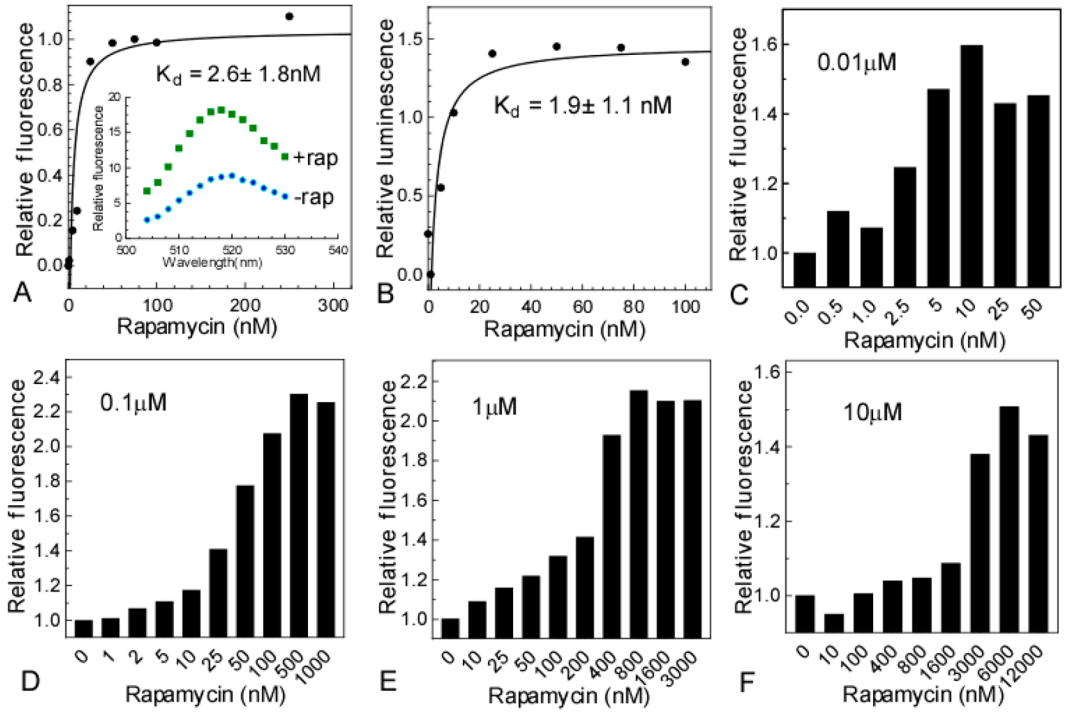

Figure 4. Light emitting two-component biosensors with caged-activators. (A) Changes in fluorescence intensity of a mixture of 50 nM of CaM-mNeonFP-FKBP and 1 μM FRB-lowCaM-M13 titrated with increasing concentrations of rapamycin. The relative fluorescence of the resulting mixtures was plotted against rapamycin concentrations and fitted to a quadratic equation leading to a K_d value of 2.6 ± 1.8 nM. The inset shows the emission scan of the same mixture with and without saturating concentrations of rapamycin. The $\lambda_{ex/em}$ values were 480 and 518 nm, respectively. (B) Changes in luminescence of a mixture of 10 nM of CaM-NanoLuc-FKBP and 1 μM FRB-mediumCaM-M13 titrated with the increasing concentration of rapamycin. The relative luminescence of the resulting mixtures was plotted against rapamycin concentrations and fitted to a quadratic equation leading to a K_d of 1.9 ± 1.1 nM. (C) Response of 0.01 μM, mNeon based rapamycin biosensor to different concentrations of its ligand; (D) as in panel C but at 0.1 μM of component concentrations; (E) as in panel C but at 1 μM of component concentrations; (F) as in panel C but at 10 μM of component concentrations. The $\lambda_{ex/em}$ values were 480 and 518 nm, respectively.

fashion increased with linker length, with 25−30 amino acid linkers deemed optimal for further engineering (Figure 2B and Figure S6). FRB-lowCaM-M13 displayed faster activating kinetics compared to other variants, and was chosen for further analysis. To test if introduction of the high affinity CaM-BP and cage assembly had an effect on overall performance of the system, we titrated a fixed amount of the biosensor with the increasing concentrations of rapamycin (Figure 2C). The fit of the initial rates of the reactions were used to obtain the K_d value of 9 ± 3.2 nM for biosensor affinity for the rapamycin, which is close to that previously observed for the uncaged version of the system (Figure 2D).[12] This confirms that introduced changes in the structure of the activation domain have not fundamentally changed the way a two-component system behaved.

Next we wanted to test the ability of the two-component biosensor with caged activator architecture to operate at high concentration of the components and analyte. To this end we tested the above-described rapamycin biosensor at component concentrations ranging from 1 to 10 μM. As can be seen in

https://dx.doi.org/10.1021/acssynbio.9b00500
ACS Synth. Biol. 2020, 9, 1306−1314

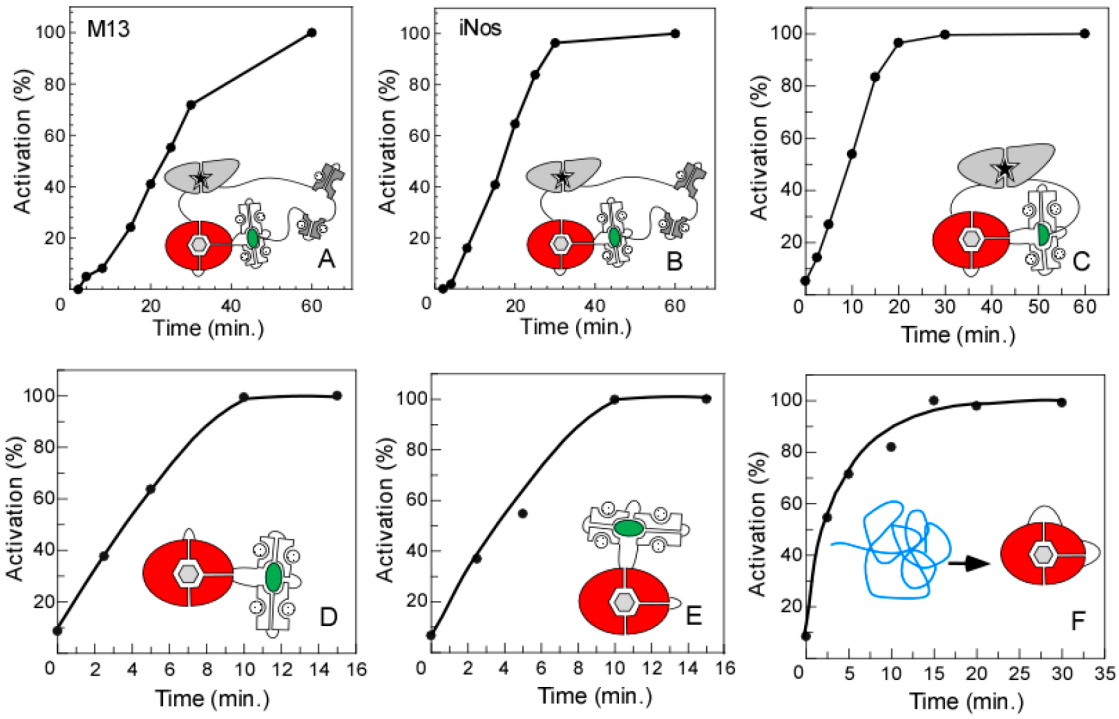

Figure 5. Time course analysis of CaM-GDH in context of a caged biosensor or directly by CaM-BP. The GDH activity of 10 nM solution of CaM-GDH-FKBP and 1 μM of (A) FRB-lowCaM-M13 or (B) FRB-lowCaM-iNOS and 0.5 μM of rapamycin that were incubated for indicated periods of time before activity was measured. (C) Time dependent activation of a solution of 10 nM of GDH-CaM-FKBP mixed with 30 nM of FRB fused to low affinity CaM-BP in the presence of rapamycin. (D) Time-resolved GDH activity of a 10 nM solution of CaM-GDH fusion following addition of 1 μM of M13 peptide. (E) As in panel D but using a fusion of CaM at a different site of GDH. (F) The rate of activation of denatured wild type GDH diluted to 0.25 nM concentration into GDH assay buffer. The functional elements of the schematics are colored as in figure A.

Figure 3 the biosensor was able to perform across concentrations tested. It is important to note that the uncaged rapamycin biosensor completely loses the ligand response at 1 μM concentration (Figure 1I). Although we observed a decrease of the dynamic range we also had to modify the assay conditions at different concentrations to prevent instant consumption of the glucose by high concentrations of biosensor. Therefore, we reduced the concentration of the PQQ cofactor in assays with 1 and 10 μM biosensor concentrations which makes the comparison between conditions more complicated due to the changes in the catalytic rates of the reporters.

As analyte-mediated dimerization is the driving force in biosensor activation, we expected the developed sensor architecture to be generally applicable. To evidence that we constructed a biosensor for another immunosuppressant drug, tacrolimus, which forms a quaternary complex with FKBP and calcineurin A/B, we produced a complex of calcineurin-A in a fusion with of calcineurin-B linked to lowCaM-CaM-BP calmodulin via 28 amino acid linker. When a solution of this recombinant protein was mixed with CaM-GDH-FKBP and titrated with tacrolimus, we detected a dose-dependent increase in GDH activity (Figure 3D), demonstrating that biosensors of molecules other than rapamycin could be constructed using the developed biosensor architecture. The fit of the data resulted in a K_d value close to that observed previously using the biosensors with the same ligand binding domains.[12]

Application of Caged-CaM-BP Activators to Light Emitting Reporter Systems. The developed caged two-component biosensor architecture is expected to be applicable to other synthetic allosteric reporters operated by calmodulin. We have previously developed CaM-fluorescent protein and CaM-NanoLuciferase switch modules and used them for construction of two-component biosensor systems.[12] Such systems are particularly attractive for construction of *in vivo* biosensors and imaging tools. Moreover, localization of the biosensor components in or on intracellular organelles may also significantly influence their local concentrations. Hence the concentration independence would be a significant advantage as the intracellular concentrations of the biosensor components are much harder to control. To test the ability of the caged CaM activators to overcome concentration dependence we constructed a CaM-NanoLuciferase (CaM-NLuc) and CaM-mNeonGreen (CaM-Neon, unpublished) fusion with FKBP domain. The recombinant proteins were mixed with the FRB-mediumCaM-M13 and FRB-lowCaM-M13 fusions, respectively, and titrated with the increasing concentrations of rapamycin. As shown in Figure 4A,B, both reporter proteins displayed dose-dependent response to rapamycin, indicating that the caged-activators are compatible with all CaM-operated chimeras. We then compared the changes of the dynamic range in the NanoLuc rapamycin biosensor operated by an uncaged or caged activator component at concentrations of 30 nM and 1 μM. An increase of concentration of the activator resulted in a 116% decrease of dynamic range in the case of the uncaged activator, while under identical conditions the caged component displayed a dynamic range reduction of 50% (Figure S8). In order to further corroborate our findings we wanted to perform the test on a system that did not require an exogenous substrate and underwent fewer time-dependent activity changes. We therefore repeated rapamycin titration

https://dx.doi.org/10.1021/acssynbio.9b00500
ACS Synth. Biol. 2020, 9, 1306−1314

experiments using different concentrations of mNeon-based rapamycin biosensor.

As shown in Figure 4 the biosensors were able to maintain responsiveness to the ligand across 3 orders of magnitude of component concentration. This also suggests that reduction of the dynamic range of the GDH and NanoLuc based biosensors detected above may be additionally influenced by inevitable variations in the assay conditions rather than the biosensor's performance.

The Relationship between the CaM-BP Sequence and Its Effect on CaM-Controlled Synthetic Switches. Calmodulin insertion is an effective strategy for converting constitutively active enzymes into allosteric switch modules.[12,11] However, the exact details of the molecular mechanism that controls CaM-BP-operated switches remains unclear, making optimization of the system an empirical process. Mammalian calmodulin can bind more than 300 peptides often with little sequence similarity, and the resulting complexes often adopt very different conformations.[13] This begs a question on whether the originally chosen M13 CaM-BP peptide is the optimal ligand for all CaM-reporter chimers and to what extent transition to caged architecture affects its suitability. We therefore decided to test a set of peptides in the caged two-component GDH based biosensor architecture. For this we chose several calmodulin peptide ligands capable of activating CaM-GDH fusion, and constructed variants of the caged rapamycin biosensor where M13 peptide was replaced by the peptides from the chosen subset (Figures S9, S10A,B,C and Tables S1 and S2). Four out of the six caged-activators induced large reporter activity changes in response to rapamycin (Figure S11). The BP2-based activator displayed high background activation even without rapamycin possibly indicating that BP2 is not efficiently sequestered by the calmodulin mutant cage. Surprisingly, unlike its uncaged form the fused version of BP11 displayed smaller signal change possibly indicating high affinity toward the mutant calmodulin or a kinetic mismatch of the system.

Activation Kinetics of Two-Component Biosensors Based on CaM-GDH. One of the advantages of protein-based signaling systems is their ability to respond to the changes in the activator concentration much faster than the gene expression-based circuits. We therefore wanted to analyze the kinetics of activation of the developed biosensors. To this end we mixed the components of the M13 and iNOS based caged rapamycin biosensors with an excess of rapamycin and incubated them for up to 60 min. At defined intervals aliquots of the reactions were withdrawn and transferred to a cuvette containing glucose, electron mediator, and the electron accepting dye, and the GDH activity was monitored. When the observed reaction rates were plotted against incubation time it transpired that iNOS-based system FRB-lowCaM-iNOS achieves maximal activation within 30 min of incubation, whereas FRB-lowCaM-M13 achieved only 70% of activation in 30 min (Figure 5A,B).

The observed biosensor activation rates are comparatively slow given that formation of the FRB and FKBP complex in the presence of rapamycin is expected to come to an equilibrium within several seconds under the assay conditions, and hence is unlikely to be a rate limiting step.[14] Two processes are likely be major contributors to the kinetics of the activation reaction: (a) the dissociation of the CaM-BP from its cage and (b) the rate of CaM-GDH structural rearrangement into active conformation after its association with CaM-BP. To distinguish between these (possibly rate limiting) steps we repeated the experiments using the uncaged version of the rapamycin biosensor.[12] As can be seen in Figure 5C, the system achieved complete activation within 30 min, indicating that while the dissociation kinetics between the CaM-cage and the CaM-BP may play a role in this process, it is unlikely to be a rate limiting step. This experiment also suggests that the differences in the activation kinetics between CaM-iNOS and CaM-M13-containing biosensors are likely to be a consequence of a particular CaM-BP/cage pairing that could be further optimized. The described biosensor system provides an ideal assay for such kinds of experiments.

As the CaM-BP/cage interactions did not appear to be the source of relatively slow biosensor response kinetics, we decided to measure the rate of activation of the core CaM-GDH switch by free CaM-BP. To this end we incubated FKBP-CaM-GDH fusion with saturating concentrations of M13 and iNOS CaM-BPs and analyzed the activity of the reaction at different time points. We found that while the core component responded to the saturating concentrations of the peptide faster than the two-component biosensors it still took nearly 10 min for the system to fully activate regardless of the activating peptide used (Figure 5D and Figure S12). The rate did not appear to be dependent on the site of CaM insertion into GDH because the earlier reported CaM-GDH switch, in which CaM was inserted in the loop connecting β-sheets 5 and 6, displayed very similar peptide activation kinetics to the variant in which CaM was inserted into loop connecting β-sheets 4 and 5 (Figure 5D,E).[12]

This is an interesting observation as the calmodulin switch is known to respond to the changes of the ligand concentration rapidly and was used to construct fluorescent biosensors of Ca^{2+} that respond on the subsecond time scale (ref 15 and references therein). Furthermore, binding of CaM-BP to CaM and isomerization of the latter is expected to be completed on the seconds scale.[16] Therefore, it is logical to assume that the observed delay is related to the structural rearrangement in GDH induced by the conformational changes of calmodulin. Given that the distance between the termini of calmodulin changes by nearly 10 Å between apo- and CaM-BP bound conformations, the perturbations of the GDH structure may range from local displacements of secondary structure to the global protein unfolding. The fact that calmodulin insertion was reliably used to create regulated OFF states in a range of proteins of unrelated structures suggests that such perturbations are large and may involve at least partial protein unfolding. Therefore, we hypothesized that the activation rate of biosensors with the CaM/CaM-BP switch may be governed by the rate of reporter refolding.

We therefore decided to assess the folding rate of the wild type GDH experimentally in order to see if it proceeds on a comparable time scale. To this end we denatured wild type GDH in 6 M guanidine hydrochloride and monitored its activity following sample dilution into buffer containing the PQQ cofactor, glucose, and the mediator/reporter dye system. As can be seen in Figure 5F the refolding was nearly quantitative and was completed within 12 min. While this does not provide a proof of the CaM-GDH functional mechanism or elucidate its rate limiting steps, it indicates that GDH folding and CaM-BP mediated activation proceed on a similar time scale. This warrants further investigation of the contribution of the reporter folding mechanism to the behavior of CaM-operated switches.

https://dx.doi.org/10.1021/acssynbio.9b00500
ACS Synth. Biol. 2020, 9, 1306−1314

DISCUSSION

One of the major challenges in understanding biology in its normal and pathological states is the requirement to monitor rapid biological processes without significantly perturbing them. While biological systems have evolved a plethora of allosteric protein modules that monitor and connect signaling and metabolic pathways, our ability to construct similarly effective and stable systems has so far been limited. We developed a strategy for construction of two-component sensing devices with input and outputs of choice. In these designs, the ligand induces changes in intermolecular proximity driving the interaction of the activator peptide, with the allosteric switch controlling the activity of the reporter enzyme. This design has the advantages of modularity and is much less influenced by the orientation of the binding domains on the analyte in the case of the fully integrated designs. However, it is strongly influenced by the concentration of the component in which at high concentrations the systems undergoes autoactivation due to the shift of the equilibrium toward the complex. To resolve this drawback we developed calmodulin mutants with reduced affinity for CaM-BP that can be used as molecular cages preventing the autoactivation of systems. Ligand mediated scaffolding of the caged CaM-BP and the reporter components led to biosensor activation across a broad range of concentrations. We demonstrate that this approach could be used to construct luminescent, fluorescent, and electrochemical biosensors of two macrocyclic peptides. Different caged systems displayed different levels of dynamic range stability across a concentration range that may, at least, in part be attributed to the changes in the assay's conditions or/and imperfect balance of the affinities of the system's components. Of note is that mNeon-based system demonstrated dynamic stability across a three-orders of magnitude concentration range which aligns well with its utilization in the *in vivo* context.

We subsequently turned our attention to factors influencing the activation kinetics of CaM-operated biosensors. Our systematic analysis revealed that the rate of activation of the core component CaM-GDH by CaM-BP is likely to be a significant contributor to the relatively slow activation rate of the biosensor. Interestingly, the activation of the CaM-GDH module proceeds with a rate very close to that of wild type GDH folding. Global and local protein unfolding is known to occur in many natural allosteric systems.[17] Conditional disordering of the proteins has been used extensively to construct protein biosensors.[18−20] Our analysis of activation kinetics suggests that the folding rate of the core enzyme component may pose the limit to how fast such a system can be activated. As proteins are not evolutionarily optimized for the rate of folding, there is likely to be room for improving the intrinsic folding rate.[21,22]

Our work demonstrates how standardized allosteric switches, activator modules, and ligand binders can be combined to create signaling systems with engineered inputs and outputs. We show that duplication of the switch component endows the system with new properties and ameliorates the problems related to concentration sensitivity. Although the presented designs rely on the conformational switching of the calmodulin molecule, similar systems can be designed using other peptide binding domains with large conformational changes. The resulting signaling modules have potential applications in bioengineering, therapeutics, and diagnostics. Particularly in the latter case, GDH-based biosensors hold the promise of creating novel point-of-care applications by utilizing commoditized glucose monitoring platforms based on electrochemical monitoring of glucose dehydrogenase activity. Here, availability of the developed biosensor architecture, deployable across a broad range of analyte concentrations using homogeneous assays, is expected to be very valuable.

MATERIAL AND METHODS

DNA Construction of Chimeric Genes. The chimeric genes were either generated by PCR or purchased as synthetic gBlocks from Integrated DNA Technologies and assembled by the Gibson Assembly method according to the manufacturer's instructions (New England Biolabs) and cloned into pET28a vector (see Table S1 for sequences).

Expression and Purification of Chimeric Proteins. Expression and purification of ligand-binding domain fused to different reporter proteins were described elsewhere.[12] All the ligand-binding domain fused caged activators were overexpressed in *E. coli* BL21(DE3)-RIL cells. Cells were grown at 37 °C, and expression was induced overnight at 18 °C in the presence of 0.3 mM isopropyl thio-β-D-galactoside (IPTG). Proteins were purified by Ni-NTA chromatography (HIS-Trap FF, ÄKTA Express Purifier, GE Healthcare) at 4 °C. The column was equilibrated with 20 mM Tris-HCl, 300 mM NaCl, 20 mM imidazole, pH 8.0. The purified protein was eluted in 20 mM Tris-HCl, 300 mM NaCl, 500 mM imidazole, pH 8.0 and dialyzed against buffer containing 20 mM Tris/HCl, pH 7.2 and 100 mM NaCl overnight. The constructs containing VHH domains were additionally purified by size exclusion chromatography on Superdex 200 column (GE Healthcare) to remove oligomers. The purified proteins were concentrated as applicable using Amicon Ultra 10K MWCO centrifugal filters (EMD Millipore, USA), and aliquoted fractions were stored at −80 °C. The protein concentration of the purified proteins were determined using Nanodrop (Thermo Fisher Scientific) using their calculated molar extinction coefficients at 280 nm based on the amino acid compositions of the final proteins by using the online tool Protparam.[23]

Spectrophotometric Analysis of PQQ-GDH Enzymatic Activity. The GDH enzyme assay was performed as described previously.[24] Briefly, the 1.0 mL volume reactions comprising 20 mM glucose, 0.6 mM phenazine methosulfate (PMS), 0.06 mM 2,6-dichlorophenylindophenol (DCPIP), 20 mM Tris-HCl, pH 7.2, 20 mM NaCl, and defined concentrations of $CaCl_2$ and enzyme were carried out in polystyrol cuvettes (SARSTEDT). The enzymatic assays were performed at 25 °C by monitoring the decrease in absorbance of DCPIP at 600 nM using a Cary 50 UV−vis absorbance spectrometer. In the assays that utilize high concentrations of biosensors, the PMS was omitted, and the concentration of PQQ was reduced to 1 nM or as indicated. This was done to bring the rate of dye reduction into the observable time frame. The exponential phase of the recorded and the exponential phase of the curves was fitted as a single exponential to obtain K_{obs}. To obtain the K_d of the interaction, the K_{obs} data were plotted against the concentration of the ligand, and the data were fitted to the explicit solution of the quadratic equation describing the E + S ⇄ ES binding equilibrium, where K_d is defined as $K_d = [E]*[S]/[EL]$. $[E_0]$ and $[L_0]$ refer to the total enzyme and

https://dx.doi.org/10.1021/acssynbio.9b00500
ACS Synth. Biol. 2020, 9, 1306−1314

ligand concentration (free and bound) in the cuvette. Under these conditions the fluorescence is described by

$$F = K_{obs(min)} + (K_{obs(max)x} - K_{obs(min)})/ *(([E_0] + [L_0] + K_d)/2 - ([E_0] + [L_0] + K_d)^2/4 - [E_0]*[L_0])^{1/2}/[L_0] \quad (1)$$

K_{obs} represents the measured rate, while $K_{obs\ (min)}$ and $K_{obs\ (max)}$ refer to the minimal and maximal rates observed, respectively. A least-squares fit of the data to eq 1 using the software package GraphPad Prism 7 was used to determine the K_d value.

GDH Refolding Assay. A 10 μL aliquot of 500 μM purified WT GDH was mixed with 90 μL of 7 M guanidinium chloride for 4 h at room temperature. Then a final 0.25 nM of denatured GDH was refolded in the buffer containing 20 mM Tris/HCl pH 7.2, 100 mM NaCl, 1 mM $CaCl_2$, and 100 nM PQQ. At the chosen refolding time, the GDH activity was measured as described above after adding a mixture containing glucose, PMS, and DCPIP.

Fluorescence Assay. The *in vitro* fluorescence titrations were carried out using a TECAN m1000 PRO plate reader. The assays were performed at 30 °C in a final volume of 200 μL containing 20 mM HEPES pH 7.5, 20 mM NaCl, 1 mM $CaCl_2$, and the indicated concentration of caged-activator. After 5 min incubation of the above to cage the activator, the 50 nM CaM-nFP (CaM-mNeon-FP) reporter and the ligand were added. After 30 min incubation time, the CaM-mNeon-FP fluorescence was excited at 480 ± 10 nm and the emission was recorded in 2 nm intervals between 500 and 530 nm. For the dynamic range calculation the peak intensity of the ligand-free (apo) state was used (518 nm) to be compared ($\Delta F/F$) with the same wavelength after the addition of the ligand.

Luciferase Assay. The 200 μL reaction volume comprising 20 mM Tris-HCl (pH 7.2), 20 mM NaCl, 1 mM $CaCl_2$, and a defined concentration of caged activators was incubated for 5 min to cage the activator, followed by the addition of 10 nM CaM-NLuc enzyme and a described amount of ligand to their final concentrations. Finally, the Nano-Glo Luciferase Assay Reagent was added, and luminescence was measured using an Infinite F500 reader (Tecan).

■ ASSOCIATED CONTENT

Supporting Information

The Supporting Information is available free of charge at https://pubs.acs.org/doi/10.1021/acssynbio.9b00500.

Summary of protein sequences used in this study; calmodulin binding peptides used in this study; additional figures to support the text; supplementary references (PDF)

■ AUTHOR INFORMATION

Corresponding Author

Kirill Alexandrov − *CSIRO-QUT Synthetic Biology Alliance, ARC Centre of Excellence in Synthetic Biology, Centre for Agriculture and the Bioeconomy, Institute of Health and Biomedical Innovation, Institute for Future Environments, School of Biology and Environmental Science, Queensland University of Technology, Brisbane, Queensland 4001, Australia;* orcid.org/0000-0002-0957-6511; Email: kirill.alexandrov@qut.edu.au

Authors

Selvakumar Edwardraja − *Institute for Molecular Biosciences, The University of Queensland, Brisbane, Queensland 4072, Australia;* orcid.org/0000-0002-4723-5152

Zhong Guo − *CSIRO-QUT Synthetic Biology Alliance, ARC Centre of Excellence in Synthetic Biology, Centre for Agriculture and the Bioeconomy, Institute of Health and Biomedical Innovation, Institute for Future Environments, School of Biology and Environmental Science, Queensland University of Technology, Brisbane, Queensland 4001, Australia*

Jason Whitfield − *Institute for Molecular Biosciences, The University of Queensland, Brisbane, Queensland 4072, Australia; CSIRO Synthetic Biology Future Science Platform, Brisbane, Queensland 4001, Australia;* orcid.org/0000-0001-5037-6389

Ignacio Retamal Lantadilla − *Institute for Molecular Biosciences, The University of Queensland, Brisbane, Queensland 4072, Australia*

Wayne A. Johnston − *CSIRO-QUT Synthetic Biology Alliance, ARC Centre of Excellence in Synthetic Biology, Centre for Agriculture and the Bioeconomy, Institute of Health and Biomedical Innovation, Institute for Future Environments, School of Biology and Environmental Science, Queensland University of Technology, Brisbane, Queensland 4001, Australia*

Patricia Walden − *CSIRO-QUT Synthetic Biology Alliance, ARC Centre of Excellence in Synthetic Biology, Centre for Agriculture and the Bioeconomy, Institute of Health and Biomedical Innovation, Institute for Future Environments, School of Biology and Environmental Science, Queensland University of Technology, Brisbane, Queensland 4001, Australia*

Claudia E. Vickers − *CSIRO Synthetic Biology Future Science Platform, Brisbane, Queensland 4001, Australia; Australian Institute for Bioengineering and Nanotechnology, The University of Queensland, Brisbane, Queensland 4072, Australia*

Complete contact information is available at: https://pubs.acs.org/10.1021/acssynbio.9b00500

Author Contributions

#S.E. and Z.G. contributed equally.

Funding

This work was supported in part by the Australian Research Council Discovery Projects DP160100973 and DP150100936 as well ITTC Grant IC160100027 and NHMRC Grant APP1113262 to K.A. This work was also in part supported by HFSP Grant RGP0002/2018 to K.A. This work was also supported by contract research funding provided by Molecular Warehouse Ltd. K.A. gratefully acknowledges financial support of QUT/CSIRO Synthetic Biology Alliance. J.W. was supported by a CSIRO Synthetic Biology Future Science Fellowship from the CSIRO Synthetic Biology Future Science Platform.

Notes

The authors declare the following competing financial interest(s): ZG and KA are named inventors on patents covering the described developments. KA is a shareholder in Molecular Warehouse Ltd that holds license to the technology described in the present publication.

■ ACKNOWLEDGMENTS

The author are grateful to Mr. Peter C. Griffin for providing venues for discussions and contemplations that led to the conceptualization of ideas underlying the present study.

REFERENCES

(1) Fenton, A. W. (2008) Allostery: An Illustrated Definition for the "Second Secret of Life. *Trends Biochem. Sci. 33* (9), 420−425.

(2) Tsai, C.-J., and Nussinov, R. (2014) A Unified View of "How Allostery Works. *PLoS Comput. Biol. 10* (2), e1003394.

(3) Guntas, G., Mansell, T. J., Kim, J. R., and Ostermeier, M. (2005) Directed Evolution of Protein Switches and Their Application to the Creation of Ligand-Binding Proteins. *Proc. Natl. Acad. Sci. U. S. A. 102* (32), 11224−11229.

(4) Kanwar, M., Wright, R. C., Date, A., Tullman, J., and Ostermeier, M. (2013) Protein Switch Engineering by Domain Insertion. *Methods Enzymol. 523*, 369−388.

(5) Ribeiro, L. F., Warren, T. D., and Ostermeier, M. (2017) Construction of Protein Switches by Domain Insertion and Directed Evolution. *Methods Mol. Biol. (N. Y., NY, U. S.) 1596*, 43−55.

(6) Amemiya, T., Koike, R., Fuchigami, S., Ikeguchi, M., and Kidera, A. (2011) Classification and Annotation of the Relationship between Protein Structural Change and Ligand Binding. *J. Mol. Biol. 408* (3), 568−584.

(7) Clark, J. J., Benson, M. L., Smith, R. D., and Carlson, H. A. (2019) Inherent versus Induced Protein Flexibility: Comparisons within and between Apo and Holo Structures. *PLoS Comput. Biol. 15* (1), 1−21.

(8) Ostermeier, M. (2009) Designing Switchable Enzymes. *Curr. Opin. Struct. Biol. 19* (4), 442−448.

(9) Nadler, D. C., Morgan, S.-A., Flamholz, A., Kortright, K. E., and Savage, D. F. (2016) Rapid Construction of Metabolite Biosensors Using Domain-Insertion Profiling. *Nat. Commun. 7*, 12266.

(10) Gräwe, A., Ranglack, J., Weyrich, A., and Stein, V. (2020) IFLinkC: An Iterative Functional Linker Cloning Strategy for the Combinatorial Assembly and Recombination of Linker Peptides with Functional Domains. *Nucleic Acids Res. 48* (4), e24.

(11) Meister, G. E., and Joshi, N. S. (2013) An Engineered Calmodulin-Based Allosteric Switch for Peptide Biosensing. *ChemBioChem 14* (12), 1460−1467.

(12) Guo, Z., Johnston, W. A., Whitfield, J., Walden, P., Cui, Z., Wijker, E., Edwardraja, S., Retamal Lantadilla, I., Ely, F., Vickers, C., et al. (2019) Generalizable Protein Biosensors Based on Synthetic Switch Modules. *J. Am. Chem. Soc. 141* (20), 8128−8135.

(13) Kursula, P. (2014) The Many Structural Faces of Calmodulin: A Multitasking Molecular Jackknife. *Amino Acids 46* (10), 2295−2304.

(14) Banaszynski, L. A., Liu, C. W., and Wandless, T. J. (2005) Characterization of the FKBP.Rapamycin.FRB Ternary Complex. *J. Am. Chem. Soc. 127* (13), 4715−4721.

(15) Farhana, I., Hossain, M. N., Suzuki, K., Matsuda, T., and Nagai, T. (2019) Genetically Encoded Fluorescence/Bioluminescence Bimodal Indicators for Ca 2+ Imaging. *ACS Sensors 4*, 1825−1834.

(16) Montigiani, S., Neri, G., Neri, P., and Neri, D. (1996) Alanine Substitutions in Calmodulin-Binding Peptides Result in Unexpected Affinity Enhancement. *J. Mol. Biol. 258* (1), 6−13.

(17) Motlagh, H. N., Wrabl, J. O., Li, J., and Hilser, V. J. (2014) The Ensemble Nature of Allostery. *Nature 508* (7496), 331−339.

(18) Dagliyan, O., Shirvanyants, D., Karginov, A. V., Ding, F., Fee, L., Chandrasekaran, S. N., Freisinger, C. M., Smolen, G. A., Huttenlocher, A., Hahn, K. M., et al. (2013) Rational Design of a Ligand-Controlled Protein Conformational Switch. *Proc. Natl. Acad. Sci. U. S. A. 110* (17), 6800−6804.

(19) Dagliyan, O., Tarnawski, M., Chu, P.-H., Shirvanyants, D., Schlichting, I., Dokholyan, N. V., and Hahn, K. M. (2016) Engineering Extrinsic Disorder to Control Protein Activity in Living Cells. *Science 354* (6318), 1441−1444.

(20) Mitrea, D. M., Parsons, L. S., and Loh, S. N. (2010) Engineering an Artificial Zymogen by Alternate Frame Protein Folding. *Proc. Natl. Acad. Sci. U. S. A. 107* (7), 2824−2829.

(21) Baker, D. (2019) What Has de Novo Protein Design Taught Us about Protein Folding and Biophysics? *Protein Sci. 28* (4), 678−683.

(22) DeGrave, A. J., Ha, J.-H., Loh, S. N., and Chong, L. T. (2018) Large Enhancement of Response Times of a Protein Conformational Switch by Computational Design. *Nat. Commun. 9* (1), 1013.

(23) Wilkins, M. R., Gasteiger, E., Bairoch, A., Sanchez, J. C., Williams, K. L., Appel, R. D., and Hochstrasser, D. F. (1998) Protein Identification and Analysis Tools in the ExPASy Server. *Methods Mol. Biol. 112*, 531−552.

(24) Yu, Y., Wei, P., Zhu, X., Huang, L., Cai, J., and Xu, Z. (2012) High-Level Production of Soluble Pyrroloquinoline Quinone-Dependent Glucose Dehydrogenase in Escherichia Coli. *Eng. Life Sci. 12* (5), 574−582.

https://dx.doi.org/10.1021/acssynbio.9b00500
ACS Synth. Biol. 2020, 9, 1306−1314